

Time-Dependent Density Functional Tight Binding: New Formulation and Benchmark of Excited States


Fabio Trani,^{*,†,‡} Giovanni Scalmani,[¶] Guishan Zheng,[§] Ivan Carnimeo,^{†,‡} Michael J. Frisch,[¶] and Vincenzo Barone^{†,‡}

[†]Scuola Normale Superiore, Piazza dei Cavalieri 7, 56126, Pisa, Italy

[‡]INFN Sezione di Pisa, Pisa, Italy

[¶]Gaussian, Inc., 340 Quinncipiac Street, Building 40, Wallingford, Connecticut 06492, United States

[§]Department of Chemistry and Chemical Biology, Harvard University, Cambridge, Massachusetts 02138, United States

 Supporting Information

ABSTRACT: A new formulation of time-dependent density functional tight binding (TD-DFTB) is reported in this paper. It is derived from the application of the linear response theory to the ground state DFTB Hamiltonian, without the introduction of additional parameters for the description of the excited states. The method is validated for several sets of organic compounds, against the best theoretical estimates from the literature, density functional theory, semiempirical methods, and experimental data. The comparison shows that TD-DFTB gives reliable results both for singlet and triplet excitation energies. In addition, the application of TD-DFTB to open-shell systems shows promising results.

1. INTRODUCTION

Thanks to ongoing developments in hardware, software, and physical models, very reliable results can be obtained for the structure and properties of small- to medium-sized molecules both in their ground state and in excited electronic states. The situation is more involved for large flexible molecules, where some degree of approximation is probably unavoidable. Here, methods rooted in density functional theory (DFT) have revolutionized the situation, paving the way toward a general purpose approach with semiquantitative accuracy along the whole periodic table without the need for prohibitively large basis sets. The subsequent development of the time-dependent (TD-DFT) route to excited electronic states^{1–5} has further enlarged the field of application of quantum-mechanical (QM) approaches. Of course, a number of problems remain to be solved (e.g., true multireference states, charge transfer, van der Waals interactions, etc.),^{6–9} and the development of improved functionals represents a very active research field.^{10–13} The recent literature has shown that, when coupled with suitable functionals (especially hybrid and/or long-range corrected models), the TD-DFT approach provides very good results.^{14–16} The recent availability of TD-DFT analytical gradients both in the gas phase and in solution provides direct access to the structure and properties of excited electronic states at a reasonable computational cost.^{17–19}

However, despite the development of linear scaling methods and other effective techniques, the large systems (with hundreds to thousands of atoms) of biological and technological interest are still highly expensive in terms of computational time. This has stimulated the development, validation, and systematic application of a semiempirical form of density functional theory, i.e., the density functional tight binding method (DFTB),^{20–25} which is several orders of magnitude faster than DFT in practical

calculations. The performances of DFTB for electronic ground states have been well characterized and benchmarked against DFT by several groups.^{26–29} In general, DFTB can well reproduce DFT geometry and energetics, its success being particularly appealing for combined quantum mechanical and molecular mechanics applications.^{30–32} This has stimulated further theoretical developments and more robust parametrizations for wider parts of the periodic table aimed at enlarging the range of application of DFTB.^{33–35}

Motivated by the effectiveness of DFTB and the good performances of TD-DFT, we have developed a new formulation of time-dependent density functional tight binding (TD-DFTB) based on the linear response approach. The scheme is naturally derived from the DFTB equations, and it does not require the introduction of additional parameters, at variance with a previous implementation of the method.³⁶ The present approach has been applied to the calculation of singlet and triplet vertical excitation energies for a benchmark set of organic molecules well studied in the literature.³⁷ The outcomes are then compared with available results of other semiempirical quantum mechanical methods, TD-DFT with different functionals, as well as *ab initio* schemes. In particular, to better understand the difference between DFTB and other semiempirical approaches, TD-PM3 and CIS-PM3 have been performed for the calculations of singlet and triplet excitation energies. The results for a few test molecules are collected and discussed toward experimental data.

In the first section, the DFTB formulation for the ground state is shortly reviewed, followed by the derivation of the TD-DFTB equations. Then, the results for the singlet and triplet excited states of a set of benchmark molecules are reported in

Received: July 4, 2011

Published: September 01, 2011

comparison with the best theoretical estimations from the literature. Statistics for these results are then summarized, and the conclusions are traced, on the basis of the benchmark results.

2. METHOD

In this section, we propose a novel formulation of TD-DFTB based on the linear response approach applied to the DFTB ground state, which is the natural extension of DFTB to the calculation of the excited states. At variance with a previous implementation,³⁶ the present approach (i) does not require the introduction of new or modified parameters and (ii) can be applied to the calculation of excited states of open-shell ground state systems. This makes TD-DFTB a very powerful and computationally affordable method, which can be used in the study of the spectroscopic properties of molecules, nanostructures, and solid crystals. In the following, the derivation of TD-DFTB is presented in detail.

The ground state DFTB total energy is typically written as

$$E = \sum_{i\sigma} \langle \psi_i^\sigma | H^0 | \psi_i^\sigma \rangle + \frac{1}{2} \sum_{AB} \gamma_{AB} \Delta q_A \Delta q_B + \frac{1}{2} \sum_{All'} p_{Al} W_{All'} p_{Al'} + \frac{1}{2} \sum_{A \neq B} V_{AB} \quad (1)$$

where ψ_i^σ is the i th occupied molecular orbital (MO) of spin σ , H^0 is the effective core Hamiltonian, and γ_{AB} is a parametrized distance-dependent function²¹ that accounts for the Coulomb interaction between the net atomic charges Δq_A and Δq_B located on atoms A and B . The third term on the right-hand side corresponds to the energy contribution from the atomic spin-densities p_{Ab} , which are partitioned according to the value of the angular momentum l and interact through a one-center atomic parameter $W_{All'}$. This contribution was not included in the initial formulation of DFTB and was introduced to account for spin densities and to be able to compute hyperfine coupling constants, effectively allowing for unrestricted calculations within DFTB.³⁸ Finally, V_{AB} is a parametrized pairwise interatomic repulsion potential. As other semiempirical methods,^{39–41} each MO is expanded in a valence minimal basis set of atomic orbitals (AO) (χ_μ)

$$\psi_i^\sigma = \sum_\mu c_{\mu i}^\sigma \chi_\mu \quad (2)$$

According to the usual linear combination of atomic orbital (LCAO) scheme, the spin-dependent density matrix and the charge and spin atomic populations are defined as

$$P_{\mu\nu}^\sigma = \sum_i c_{\mu i}^\sigma c_{\nu i}^\sigma \quad (3)$$

$$\Delta q_A = q_A - Z_A = \left[\sum_{\mu \in A} \sum_\nu (P_{\mu\nu}^\alpha + P_{\mu\nu}^\beta) S_{\mu\nu} \right] - Z_A \quad (4)$$

$$p_{Al} = \sum_{\mu \in Al} \sum_\nu (P_{\mu\nu}^\alpha - P_{\mu\nu}^\beta) S_{\mu\nu} \quad (5)$$

where $S_{\mu\nu}$ are the elements of the overlap matrix and Z_A is the valence nuclear charge of atom A . The ground state DFTB energy in eq 1 is variationally minimized with respect to the LCAO coefficients $c_{\mu i}^\sigma$ using the Kohn–Sham independent particle approximation, and the associate one-particle Fock matrix is defined as

$$F_{\mu\nu}^\sigma = \frac{\partial E}{\partial P_{\mu\nu}^\sigma} = h_{\mu\nu} + G_{\mu\nu}^\sigma \quad (6)$$

where $h_{\mu\nu}$ are the elements of the one-electron operator

$$h_{\mu\nu} = h_{\mu\nu}^0 - \frac{1}{2} S_{\mu\nu} \left[\sum_C (\gamma_{AC} + \gamma_{BC}) Z_C \right] \quad (7)$$

involving the parametrized effective core Hamiltonian matrix elements $h_{\mu\nu}^0$ and the nuclear attraction terms. Both $h_{\mu\nu}^0$ and $S_{\mu\nu}$ are parametrized in DFTB either starting from molecular systems or from bulk reference systems.²¹ The terms in square brackets arise from the interaction between the valence nuclear charge Z_C of atom C and the electron charge density.³⁰

The charge–charge and spin–spin interactions in eq 1 are both quadratic in the density matrix, and they give rise to the two-electron term $G_{\mu\nu}^\sigma$, which can be partitioned into Coulomb- and exchange-like interaction terms

$$G_{\mu\nu}^\sigma = J_{\mu\nu} + K_{\mu\nu}^\sigma \quad (8)$$

where

$$J_{\mu\nu} = \frac{1}{2} S_{\mu\nu} \left[\sum_C (\gamma_{AC} + \gamma_{BC}) q_C \right] \quad (9)$$

$$K_{\mu\nu}^\sigma = \frac{1}{2} \delta_\sigma S_{\mu\nu} \left[\sum_{Cl'l''} (\delta_{AC} W_{Cl'l''} + \delta_{BC} W_{Cl'l''}) p_{Cl''} \right] \quad (10)$$

where $\delta_\sigma = \delta_{\sigma\sigma} - \delta_{\sigma\beta}$ (δ_{ij} is the Kronecker delta). The μ and ν AOs are centered on A and B atoms and have l and l' angular momenta, respectively.

In order to apply a linear response approach to the DFTB ground state, it is better to identify the four-index kernels corresponding to the Coulomb and exchange interaction terms,¹⁹ through the second derivatives of the DFTB total energy (eq 1) with respect to the density matrix elements

$$\frac{\partial^2 E}{\partial P_{\mu\nu}^\sigma \partial P_{\kappa\lambda}^{\sigma'}} = J_{\mu\nu\kappa\lambda} + K_{\mu\nu\kappa\lambda}^{\sigma\sigma'} \quad (11)$$

By using a permutation-invariant expression of the total energy derivatives (based on the symmetry properties of the ground state density matrix), the four-index kernels can be written according to the following symmetric form:

$$J_{\mu\nu\kappa\lambda} = \frac{1}{4} S_{\mu\nu} (\gamma_{AC} + \gamma_{BC} + \gamma_{AD} + \gamma_{BD}) S_{\kappa\lambda} \quad (12)$$

$$K_{\mu\nu\kappa\lambda}^{\sigma\sigma'} = \frac{1}{4} \delta_\sigma \delta_{\sigma'} S_{\mu\nu} (W_{All''} \delta_{AC} + W_{Bl'l''} \delta_{BC} + W_{All''' } \delta_{AD} + W_{Bl'l''' } \delta_{BD}) S_{\kappa\lambda} \quad (13)$$

where the μ , ν , κ , and λ AOs are respectively located on A , B , C , and D atoms, and have l , l' , l'' , and l''' angular momenta. Since DFTB is derived from a second-order Taylor expansion of the density functional total energy with respect to electron density fluctuations, the DFTB energy can be eventually written as

$$E = \sum_{\sigma} \sum_{\mu\nu} h_{\mu\nu} P_{\mu\nu}^\sigma + \frac{1}{2} \sum_{\sigma\sigma'} \sum_{\mu\nu\kappa\lambda} [J_{\mu\nu\kappa\lambda} + K_{\mu\nu\kappa\lambda}^{\sigma\sigma'}] P_{\mu\nu}^\sigma P_{\kappa\lambda}^{\sigma'} + \frac{1}{2} \sum_{A \neq B} (V_{AB} + Z_A \gamma_{AB} Z_B) \quad (14)$$

The application of the linear response theory to DFTB is straightforward, and it is equivalent to the corresponding derivation within TD-DFT (see, for example, ref 42). The final equations are typically written in superoperator form as a non-Hermitian eigenvalue problem:

$$\begin{pmatrix} \mathbf{A} & \mathbf{B} \\ \mathbf{B} & \mathbf{A} \end{pmatrix} \begin{pmatrix} \mathbf{X} \\ \mathbf{Y} \end{pmatrix} = \Omega \begin{pmatrix} 1 & 0 \\ 0 & -1 \end{pmatrix} \begin{pmatrix} \mathbf{X} \\ \mathbf{Y} \end{pmatrix} \quad (15)$$

where the Ω 's are the excitation energies and the eigenvectors comprise the single excitation $X_{ai} = \delta P_{ai}$ and de-excitation $Y_{ai} = \delta P_{ia}$ amplitudes.⁴² Note that we are using the conventional notation where i, j, \dots are occupied MOs while a, b, \dots are virtual MOs. The elements of the \mathbf{A} and \mathbf{B} matrices are defined as

$$A_{ai\sigma, bj\sigma'} = (\varepsilon_{a\sigma} - \varepsilon_{i\sigma}) \delta_{ab} \delta_{ij} \delta_{\sigma\sigma'} + \frac{\partial F_{ai}^{\sigma}}{\partial P_{bj}^{\sigma'}} \quad (16)$$

$$B_{ai\sigma, bj\sigma'} = \frac{\partial F_{ai}^{\sigma}}{\partial P_{jb}^{\sigma'}} \quad (17)$$

and they involve the ground state orbital energies $\varepsilon_{p\sigma}$. The matrix operator on the left-hand side of eq 15 is typically diagonalized using an iterative scheme, in which the four-index matrices $(\mathbf{A} + \mathbf{B})$ and $(\mathbf{A} - \mathbf{B})$ are evaluated in the AO basis and contracted with the $(\mathbf{X} + \mathbf{Y})$ and $(\mathbf{X} - \mathbf{Y})$ combinations of single excitation amplitudes, once transformed into the AO basis.⁴² Note that in the AO basis, the $(\mathbf{A} + \mathbf{B})_{\mu\nu\sigma\kappa\lambda\sigma'}$ matrix is symmetric with respect to $\mu \leftrightarrow \nu$ and $\kappa \leftrightarrow \lambda$, while the $(\mathbf{A} - \mathbf{B})_{\mu\nu\sigma\kappa\lambda\sigma'}$ is antisymmetric with respect to the same index permutations. Moreover, $(\mathbf{X} + \mathbf{Y})_{\mu\nu\sigma}$ and $(\mathbf{X} - \mathbf{Y})_{\mu\nu\sigma}$ are symmetric and antisymmetric to the $\mu \leftrightarrow \nu$ permutation, respectively. By carrying out the Fock matrix derivatives in eqs 16 and 17 in the AO basis, it is easy to realize that $(\mathbf{A} + \mathbf{B})_{\mu\nu\sigma\kappa\lambda\sigma'}$ involves both charge and the symmetric component of spin interaction kernels:

$$\begin{aligned} (\mathbf{A} + \mathbf{B})_{\mu\nu\sigma\kappa\lambda\sigma'} &\leftarrow (\mathbb{J}_{\mu\nu\kappa\lambda} + \mathbb{J}_{\mu\nu\lambda\kappa}) + (\mathbb{K}_{\mu\nu\kappa\lambda}^{\sigma\sigma'} + \mathbb{K}_{\mu\nu\lambda\kappa}^{\sigma\sigma'}) \\ &= 2\mathbb{J}_{\mu\nu\kappa\lambda} + (\mathbb{K}_{\mu\nu\kappa\lambda}^{\sigma\sigma'} + \mathbb{K}_{\mu\nu\lambda\kappa}^{\sigma\sigma'}) \end{aligned} \quad (18)$$

while $(\mathbf{A} - \mathbf{B})_{\mu\nu\sigma\kappa\lambda\sigma'}$ involves only the antisymmetric component of the spin interaction kernel:

$$\begin{aligned} (\mathbf{A} - \mathbf{B})_{\mu\nu\sigma\kappa\lambda\sigma'} &\leftarrow (\mathbb{J}_{\mu\nu\kappa\lambda} - \mathbb{J}_{\mu\nu\lambda\kappa}) + (\mathbb{K}_{\mu\nu\kappa\lambda}^{\sigma\sigma'} - \mathbb{K}_{\mu\nu\lambda\kappa}^{\sigma\sigma'}) \\ &= (\mathbb{K}_{\mu\nu\kappa\lambda}^{\sigma\sigma'} - \mathbb{K}_{\mu\nu\lambda\kappa}^{\sigma\sigma'}) \end{aligned} \quad (19)$$

It is somewhat difficult to understand why the spin interaction kernel has a nonzero antisymmetric component, and therefore an example system only involving the four AO basis functions μ_{Ab} , $\nu_{B'l'}$, $\kappa_{A'l''}$, and $\lambda_{B'l''}$ is given below (subscripts are used to indicate the atom where they are located and their angular momentum label). The two spin interaction kernels corresponding to the $\kappa \leftrightarrow \lambda$ permutation are derived from the general case in eq 13 as

$$\mathbb{K}_{\mu\nu\kappa\lambda}^{\sigma\sigma'} = \frac{1}{4} \delta_{\sigma} \delta_{\sigma'} S_{\mu\nu} (W_{A'l''} + W_{B'l''}) S_{\kappa\lambda} \quad (20)$$

$$\mathbb{K}_{\mu\nu\lambda\kappa}^{\sigma\sigma'} = \frac{1}{4} \delta_{\sigma} \delta_{\sigma'} S_{\mu\nu} (W_{A'l''} + W_{B'l''}) S_{\lambda\kappa} \quad (21)$$

and they are graphically depicted in Figure 1. The expressions in eqs 20 and 21 correspond to the following contribution to the

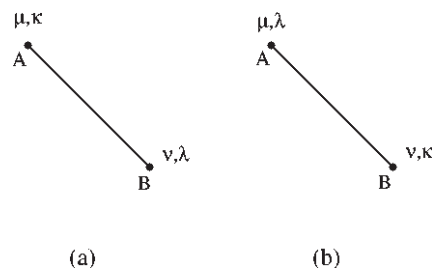


Figure 1. Exchange contributions from the $\mathbb{K}_{\mu\nu\kappa\lambda}^{\sigma\sigma'}$ and $\mathbb{K}_{\mu\nu\lambda\kappa}^{\sigma\sigma'}$ terms, respectively, when the atomic orbitals are centered on atoms A and B.

$(\mathbf{A} + \mathbf{B})_{\mu\nu\sigma\kappa\lambda\sigma'}$ and $(\mathbf{A} - \mathbf{B})_{\mu\nu\sigma\kappa\lambda\sigma'}$ matrices:

$$\begin{aligned} (\mathbf{A} + \mathbf{B})_{\mu\nu\sigma\kappa\lambda\sigma'} &\leftarrow (\mathbb{K}_{\mu\nu\kappa\lambda}^{\sigma\sigma'} + \mathbb{K}_{\mu\nu\lambda\kappa}^{\sigma\sigma'}) \\ &= \frac{1}{4} \delta_{\sigma} \delta_{\sigma'} S_{\mu\nu} (W_{A'l''} + W_{A'l'''} + W_{B'l'l''} + W_{B'l'l'''}) S_{\kappa\lambda} \end{aligned} \quad (22)$$

$$\begin{aligned} (\mathbf{A} - \mathbf{B})_{\mu\nu\sigma\kappa\lambda\sigma'} &\leftarrow (\mathbb{K}_{\mu\nu\kappa\lambda}^{\sigma\sigma'} - \mathbb{K}_{\mu\nu\lambda\kappa}^{\sigma\sigma'}) \\ &= \frac{1}{4} \delta_{\sigma} \delta_{\sigma'} S_{\mu\nu} (W_{A'l''} - W_{A'l'''} - W_{B'l'l''} + W_{B'l'l'''}) S_{\kappa\lambda} \end{aligned} \quad (23)$$

where we used the fact that $S_{\kappa\lambda}$ itself is indeed symmetric with respect to the $\kappa \leftrightarrow \lambda$ permutation.

In principle, DFTB is derived from a DFT formalism with a pure exchange-correlation functional, which depends only locally on the density⁴³ (and other density-related quantities like the density gradient etc). In other words, DFTB is derived without the inclusion of nonlocal Hartree–Fock exact exchange, and therefore, just as in the case of TD-DFT using pure functionals, the $(\mathbf{A} - \mathbf{B})_{\mu\nu\sigma\kappa\lambda\sigma'}$ matrix should be strictly diagonal.⁴² The previously published formulation of TD-DFTB³⁶ is consistent with this observation because the on-site spin–spin interaction parameters W_A used in that paper are scalars, which do not depend on the AO angular momentum. Under these conditions, $(\mathbf{A} - \mathbf{B})_{\mu\nu\sigma\kappa\lambda\sigma'}$ does remain strictly diagonal since eqs 20 and 21 become identical, and the right-hand side of eq 23 vanishes. However, the parameters being used for the spin–spin interaction in an, e.g., a triplet excited state computed as an excitation from a closed-shell singlet are not the same that would have been used if that triplet was computed using the open-shell formulation of DFTB for the ground state³⁸ (where the $W_{A'l'}$ are not scalars, as they depend on the AO angular momentum).

To summarize, in this section, we have shown how to apply the linear response approach to an unrestricted ground state DFTB calculation. The resulting TD-DFTB method does not require additional or modified spin–spin parameters, and it is applicable to both closed- and open-shell ground states. Notably, in our formulation of TD-DFTB, the $(\mathbf{A} - \mathbf{B})_{\mu\nu\sigma\kappa\lambda\sigma'}$ matrix is not diagonal, just like what happens in the case of TD-DFT when an hybrid functional is used, i.e., when a fraction of the nonlocal Hartree–Fock exact exchange is present. Indeed, this suggests that the open-shell formulation of DFTB which involves orbital angular momentum dependent spin–spin parameters $W_{A'l'}$ could be already regarded as a model derived from a hybrid DFT formalism which involves the exact exchange.

Table 1. Sets of Organic Compounds Used for Benchmark

group I	group II	group III	group IV
ethene	benzene	formaldehyde	cytosine
E-butadiene	naphthalene	acetone	thymine
all-E-hexatriene	furan	p-benzoquinone	uracil
all-E-octatetraene	pyrrole	formamide	adenine
cyclopropene	imidazole	acetamide	
cyclopentadiene	pyridine	propanamide	
norbornadiene	pyrazine		
	pyrimidine		
	pyridazine		
	s-triazine		
	s-tetrazine		

3. RESULTS

The method described in the previous section has been used to calculate the excitation energies in the benchmark set of organic compounds proposed by Thiel and co-workers.³⁷ In that paper, the authors collected the Theoretical Best Estimates (TBEs) for both singlet and triplet vertical excitation energies calculated at the CASPT2 level with a molecular structure optimized at the MP2 level. The same sets of compounds and excitations have been used to benchmark the accuracy of multireference Configuration Interaction (CI) approaches,¹⁵ TD-DFT (by assessing the performance of many exchange-correlation functionals),^{16,44,45} and semiempirical quantum chemical methods.⁴⁶ For this reason, the same four sets of compounds and excitations are used in this paper as a benchmark for the TD-DFTB scheme. The compounds are divided into four groups, as summarized in Table 1. Group I contains unsaturated aliphatic hydrocarbons; group II, aromatic hydrocarbons and heterocycles; group III, aldehydes, ketones, and amides; and group IV, nucleobases.

The optimized geometries at the MP2 level were taken from the literature.³⁷ Indeed, the use of good quality MP2-optimized geometries seems to be accepted as a standard approach to benchmark the accuracy of a method for excited state calculations, since it avoids biasing the results due to the quality of the ground-state geometries provided by the method under testing. But, in order to show the good quality of the method, TD-DFTB calculations using geometries optimized at the DFTB electronic ground state were also performed. In the Supporting Information, the full set of singlet and triplet vertical excitation energies are collected, using geometries optimized both at the MP2 level and at the DFTB level.

TD-DFTB is based on a minimal orbital basis set that can only model valence excited states, while it cannot describe diffuse excitations such as Rydberg states. For this reason, the analysis was restricted to valence excited states. To better compare the method against standard semiempirical schemes, TD-PM3 and CIS-PM3 calculations on singlet and triplet excited states have been performed for a restricted set of molecules. This set has been recently used to carefully validate TD-DFT toward experimental data.⁴⁷ A comparative study of the methods (TD-PM3, TD-DFTB, TD-DFT) against TBEs and experimental data is discussed for this restricted set of molecules, before going to the statistics of TD-DFTB on the large benchmark set of molecules listed in Table 1. All calculations were performed using

TD-DFTB, TD-PM3, and CIS-PM3 implemented in the development version of the Gaussian program.⁴⁸

Singlet States. Singlet excitation energies have been computed using TD-DFTB with geometries optimized at the MP2 level. Before reporting on the statistics obtained from the benchmark set of molecules, it is interesting to compare the excitation energies obtained by TD-DFTB with the ones obtained by other semiempirical methods. The comparison is done using as a reference a recent paper where configuration interaction calculations using single, double, triple, and quadruple excitations (CISDTQ) have been proposed for standard semiempirical methods (MNDO, INDO/S, AM1, PM3) and orthogonalization-corrected approaches (OM1, OM2, OM3).⁴⁶ To better compare TD-DFTB and semiempirical approaches, we applied TD-PM3 and CIS-PM3 to calculate singlet excitation energies for a few molecules recently carefully characterized using DFT approaches.⁴⁷ The results have been collected in Table 2, where TD-DFTB is compared to TD-PM3, CIS-PM3, experimental data, TD-PBE, TD-B3LYP, TBEs, and CISDTQ-PM3.

As can be observed from the table, the singlet excitation energies calculated at the PM3 level are often strongly underestimated within TD and CIS approximation. As a matter of fact, semiempirical approaches often need a CISDTQ level of approximation for obtaining converged excitation energies, thus requiring a high degree of computational effort. Table 2 shows that, with respect to PM3, in most cases, TD-DFTB is much closer to TBE/experimental data. For instance, the excitation energy of ethene $^1B_{1u}$ is strongly underestimated within TD-PM3 (it is more than 2.0 eV below). The energy is raised when using CIS-PM3 (5.86 eV) and then CISDTQ-PM3 (6.63 eV), but even in this case, the error with respect to TBE (7.80 eV) and experimental data (7.65) is greater than 1 eV. On the other hand, the excitation energy is well reproduced by TD-DFTB (7.64 eV).

The trend TD-PM3 < CIS-PM3 < CISDTQ-PM3 < TBE/exptl is observed for ethene, E-butadiene, formaldehyde, and acetone. The situation changes for aromatic hydrocarbons, where, however, apart from a few cases, TD-DFTB performs much better than PM3. For instance, the pyrazine $^1B_{3u}$ excited state is evaluated at 3.31, 3.35 and 3.29 eV within TD-, CIS- and CISDTQ-PM3, respectively, against 3.95 eV (TBE) and 3.83 eV (experimental). At the same MP2-level optimized geometry, TD-DFTB gives a better estimate at 3.66 eV.

Standard semiempirical methods of quantum chemistry give results even worse when using PM6 instead of PM3. In particular, TD-PM6 gives 4.98 and 3.24 eV for ethene $^1B_{1u}$ and pyrazine $^1B_{3u}$ excited states, respectively, thus showing a significant underestimation of singlet excited states with respect to all other approaches here considered. From these comparisons, TD-DFTB emerges as an invaluable tool for predicting excited states of organic molecules. In the last rows of Table 2, the mean errors and standard deviations with respect the experimental data are reported. It is worth noting that these data are merely indicative since the set of considered compounds is really small. It only involves the lowest excitations, and it is unbalanced toward the aromatic hydrocarbons. For this reason, TD-DFTB appears with a small value of the signed error with respect to the experimental data. Nonetheless, Table 2 gives important information to compare in a glance the several methods for a few molecules, with respect to the experimental data. From now on, this section will focus on the larger benchmark set, composed by the compounds listed in Table 1, and more suitable for doing statistics. All of the excitation energies for the benchmark set,

Table 2. Comparison of Singlet Vertical Excitation Energies (in eV) Calculated for a Few Molecules Using Different Approaches^a

		PM3			DFTB	PBE	B3LYP		
		TD	CIS	CISDTQ	TD	TD	TD	TBE	exptl
ethene	${}^1B_{1u}(\pi \rightarrow \pi^*)$	5.68	5.86	6.63	7.64	7.07	7.32	7.80	7.65
E-butadiene	${}^1B_u(\pi \rightarrow \pi^*)$	4.60	4.78	5.45	5.49	5.41	5.54	6.18	5.91
formaldehyde	${}^1A_2(n \rightarrow \pi^*)$	2.65	2.69	2.87	4.13	3.78	3.89	3.88	4.00
	${}^1B_1(\sigma \rightarrow \pi^*)$	8.47	8.48	8.63	8.18	8.83	8.96	9.10	9.00
acetone	${}^1A_2(n \rightarrow \pi^*)$	3.08	3.12	3.29	4.38	4.20	4.36	4.40	4.43
pyridine	${}^1B_1(n \rightarrow \pi^*)$	3.75	3.79	3.75	4.49	4.34	4.78	4.59	4.59
	${}^1B_2(\pi \rightarrow \pi^*)$	4.04	4.17	3.35	5.31	5.31	5.44	4.85	4.99
	${}^1A_2(n \rightarrow \pi^*)$	4.32	4.33	3.96	4.84	4.44	5.10	5.11	5.43
	${}^1A_1(\pi \rightarrow \pi^*)$	4.28	4.34	5.00	5.77	6.17	6.23	6.26	6.38
pyrazine	${}^1B_{3u}(n \rightarrow \pi^*)$	3.31	3.35	3.29	3.66	3.55	3.94	3.95	3.83
	${}^1B_{2u}(\pi \rightarrow \pi^*)$	4.12	4.26	3.48	5.11	5.22	5.31	4.64	4.81
	${}^1B_{2g}(n \rightarrow \pi^*)$	4.09	4.13	4.13	5.39	5.11	5.56	5.56	5.46
	${}^1B_{1g}(n \rightarrow \pi^*)$	5.19	5.19	4.51	6.14	5.57	6.40	6.60	6.10
pyrimidine	${}^1B_1(n \rightarrow \pi^*)$	3.53	3.57	3.46	4.17	3.77	4.26	4.55	3.85
	${}^1A_2(n \rightarrow \pi^*)$	3.84	3.86	3.66	4.52	3.99	4.59	4.91	4.62
	${}^1B_2(\pi \rightarrow \pi^*)$	4.24	4.36	3.55	5.48	5.57	5.71	5.44	5.12
pyridazine	${}^1B_1(n \rightarrow \pi^*)$	3.14	3.18	3.15	3.51	3.11	3.56	3.78	3.60
	${}^1A_2(n \rightarrow \pi^*)$	4.36	4.40	4.16	4.94	5.02	5.46	5.77	5.30
	${}^1A_1(\pi \rightarrow \pi^*)$	4.11	4.24	3.41	5.30	5.44	5.58	5.18	5.00
s-tetrazine	${}^1B_{3u}(n \rightarrow \pi^*)$	2.32	2.36	2.27	2.39	1.83	2.24	2.29	2.25
	${}^1A_u(n \rightarrow \pi^*)$	3.26	3.30	2.99	3.56	2.80	3.48	3.51	3.40
mean error		−0.92	−0.86	−0.99	−0.06	−0.25	0.09	0.13	
std. dev.		0.54	0.52	0.50	0.34	0.38	0.29	0.25	

^a All calculations have been performed at MP2-level optimized geometries, as given in ref 37. Experimental data and TD-DFT results have been taken from Ref 47, while CISDTQ results have been taken from ref 46. At the bottom of the table, the signed mean error and the standard deviation with respect to the experimental data are reported. The last column contains the statistics on the whole set.

Table 3. Statistics for Vertical Singlet Excitation Energies (eV) Calculated within TD-DFTB for the Four Groups of Compounds, with Respect to the TBES

	group I	group II	group III	group IV	total
count	13	53	19	19	104
mean	−0.46	−0.28	−0.31	−0.90	−0.42
abs. mean	0.46	0.34	0.54	0.90	0.49
std. dev.	0.30	0.34	0.57	0.52	0.48
max + dev.	−0.05	0.47	0.61	−0.27	0.61
max − dev.	0.90	1.05	1.19	1.94	1.94

calculated within TD-DFTB, are reported in the Supporting Information.

Statistics on the four groups of compounds with respect to the TBES are reported in Table 3. The best agreement between TD-DFTB and the TBES is found for group II, i.e., for the aromatic hydrocarbons and heterocycles, while the worst agreement is undoubtedly found for the nucleobases (group IV). This is in line with the results obtained using other semiempirical quantum chemical methods, such as AM1 and PM3.⁴⁶

The results obtained using geometries optimized at both the MP2 and DFTB levels have been compared (see the Supporting Information). While excitation energies can be sometimes slightly different for the two cases, we found that overall the statistics do not change much. The signed and absolute mean

errors for excitation energies obtained using the DFTB-optimized geometries are −0.40 and 0.50 eV, in agreement with the results obtained with the MP2-optimized geometries, that are −0.42 and 0.49 eV, respectively (see Table 3).

A comparison with the results provided by a previous implementation³⁶ of the TD-DFTB method has been carried out, and a good agreement is found. The differences between the current and the previous approach are quite small, usually below 0.1 eV (see Supporting Information). As shown above, the main difference between the two schemes is in the antisymmetric contribution through the (A − B) matrices, due to the angular dependence of the spin–spin interaction parameters. The antisymmetric contribution is quite small for singlet excited states, and this justifies the observed agreement between the two different formulations of TD-DFTB.

The present results (Table 3) show that TD-DFTB tends to underestimate the excitation energies. The signed mean error (the deviation from TBE) for singlet excited states is −0.42 eV, which is consistent with the fact that the parametrization of the DFTB Fock matrix was done on the basis of DFT calculations using the PBE functional, which underestimates (on average) the singlet excitation energies of organic molecules.^{16,47}

On the other hand, TD-DFTB performs much better than CISDTQ-PM3 and -AM1, whose mean errors are −1.40 eV and −1.14 eV, respectively.⁴⁶ The present method shows a mean error larger than INDO/S2 (−0.11 eV), but in those calculations the errors appear to be spread (the standard deviation is 0.77 eV).

TD-DFTB results are less scattered with respect to the INDO results, and the standard deviation of 0.48 eV is even smaller than the one observed for OMx methods (OM3 shows a standard deviation of 0.54 eV).⁴⁶

The deviations for singlet excitation energies are shown in Figure 2. With the exception of a few cases, a systematic underestimation of the excitation energies is apparent, which can be due to the behavior of the PBE functional, which is inherited by DFTB through its parametrization. With few exceptions, TD-DFTB gives errors which are all scattered within a fairly small energy range of about 2 eV.

Triplet States. The TD-DFTB method introduced in the previous section has been benchmarked against TBEs for singlet–triplet vertical excitation energies. All of the results have been collected in the Supporting Information. In Table 4, a comparison of the method toward TD-, CIS-, and CISDTQ-PM3 for a few selected molecules is reported.

The trend $\text{TD-PM3} < \text{CIS-PM3} < \text{CISDTQ-PM3} < \text{TBE/exptl}$, observed in the previous section, is confirmed for triplet excitation energies of ethene, E-butadiene, formaldehyde, and

acetone. For instance, the ethene ${}^3B_{1u}$ excitation energy is 1.54, 2.56, and 3.05 eV, within TD-, CIS-, and CISDTQ-PM3 approximations, respectively, against the reference value of 4.50 eV (TBE). Therefore, in the best case, PM3 is about 1.5 eV below the reference value. Instead, the excitation energy reported within TD-DFTB is 5.26 eV, that is, 0.76 eV above TBE. A similar situation is observed for formaldehyde, where the best PM3 estimate of 3A_2 excitation energy, 2.57 eV, obtained within CISDTQ, is 0.93 eV below TBE/exptl (3.50 eV). TD-DFTB instead gives 4.13 eV, that is, 0.63 eV above the reference value. The same trend is observed for pyridine, while for s-tetrazine, PM3 gives better results. In fact, while for the other molecules here considered, PM3 (within all approximations) gives results well below both TBE and experimental data; for s-tetrazine, there is better agreement. Just like for singlet excitations, even for triplet excited states, a careful analysis has been performed on a large benchmark set, with the aim of getting realistic statistical data. A table containing all of the triplet excitation energies is included in the Supporting Information file.

In Table 5, the statistics on the four groups of organic compounds reported in Table 1 are summarized. A histogram with the deviations for the excitations toward triplet states is shown in Figure 3. An interesting feature of TD-DFTB emerges from this analysis. Other semiempirical approaches either show the same precision (PM3, OMx) or they perform much worse (INDO) for triplet states than for singlet states.⁴⁶ At variance with them, TD-DFTB gives better results (on average) for triplet than for singlet excited states. Indeed, the signed mean error is very small (0.07 eV). The absolute error is also smaller with respect to the singlet excitation energies, and the deviations from the TBE values are less scattered (the standard deviation is 0.43 eV). Our results indicate that while TD-DFTB quite systematically underestimates the excitation energies of singlet states, the signed deviations from the TBEs for triplet states sum up to a very small mean error.

Another interesting point of comparison is the first singlet to triplet energy difference $S_0 \rightarrow T_0$. The energy of the T_0 state can be computed in two ways: either using TD-DFTB and therefore

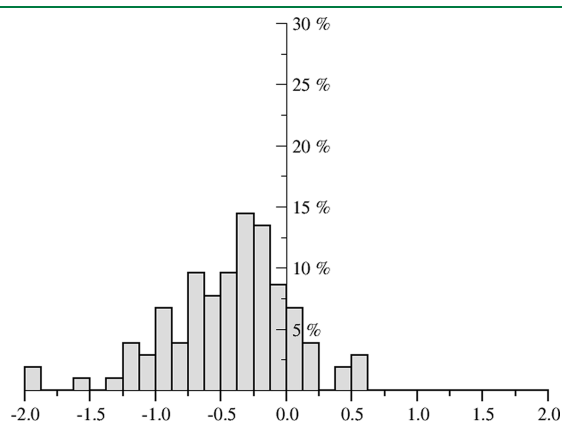


Figure 2. Histograms of the deviations for singlet vertical excitation energies (in eV) calculated by TD-DFTB with respect to the TBEs.

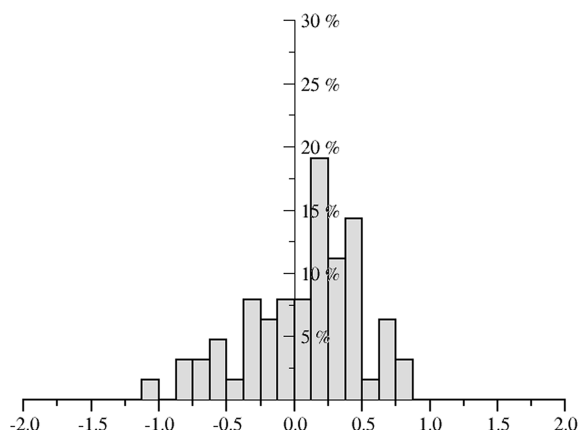
Table 4. Singlet–Triplet Vertical Excitation Energies (in eV) Calculated for a Few Molecules Using Different Approaches^a

		PM3			DFTB	PBE	B3LYP	TBE	exptl
		TD	CIS	CISDTQ	TD	TD	TD		
ethene	${}^3B_{1u}(\pi \rightarrow \pi^*)$	1.54	2.56	3.05	5.26	4.25	4.05	4.50	4.6
E-butadiene	${}^3B_u(\pi \rightarrow \pi^*)$		1.87	2.28	3.62	2.95	2.78	3.20	3.22
	${}^3A_g(\pi \rightarrow \pi^*)$	2.22	2.86	3.32	5.53	5.03	4.87	5.08	4.91
formaldehyde	${}^3A_2(\pi \rightarrow \pi^*)$	2.27	2.31	2.57	4.13	3.02	3.13	3.50	3.50
	${}^3A_1(\pi \rightarrow \pi^*)$	4.28	4.73	5.07	6.50	5.56	5.20	5.87	5.82
acetone	${}^3A_2(n \rightarrow \pi^*)$	2.72	2.76	3.05	4.38	3.55	3.69	4.05	4.16
	${}^3A_1(\pi \rightarrow \pi^*)$	3.92	4.35	4.65	6.19	5.63	5.40	6.03	5.88
pyridine	${}^3A_1(\pi \rightarrow \pi^*)$		2.42	2.68	4.77	4.14	3.90	4.06	4.10
	${}^3B_2(\pi \rightarrow \pi^*)$	3.46	3.51	3.44	4.81	4.45	4.52	4.64	4.84
s-tetrazine	${}^3B_{3u}(n \rightarrow \pi^*)$	1.77	1.84	1.88	2.39	1.09	1.42	1.89	1.69
	${}^3A_u(n \rightarrow \pi^*)$	2.86	2.92	2.80	3.56	2.48	3.10	3.52	2.90
	${}^3B_{1g}(n \rightarrow \pi^*)$	2.96	3.00	3.14	4.63	3.30	3.63	4.21	3.60
mean error		−1.39	−1.17	−0.94	0.55	−0.31	−0.29	0.11	
std. dev.		1.02	0.71	0.57	0.28	0.22	0.25	0.26	

^a All calculations have been performed at MP2-level optimized geometries, as given in ref 37. Experimental data and TBEs have been taken from ref 37. TD-PBE and TD-B3LYP calculations are from ref 44. CISDTQ results are from ref 46. At the bottom of the table, the signed mean error and the standard deviation with respect to the experimental data are reported. All values are in eV.

Table 5. Deviations in the Vertical Excitation Energies (eV) Towards Triplet States within TD-DFTB For All the Compounds in the Benchmark Set, as Compared with the TBEs

	group I	group II	group III	total
count	13	36	14	63
mean	0.37	−0.02	0.03	0.07
abs. mean	0.39	0.36	0.30	0.35
std. dev.	0.27	0.44	0.41	0.43
max + dev.	0.77	0.71	0.63	0.77
max − dev.	0.18	1.08	0.87	1.08

**Figure 3.** Histograms of the deviations for triplet vertical excitation energies (in eV) calculated by TD-DFTB with respect to the TBEs.

computing T_0 as an excited state of S_0 or by performing an unrestricted ground state DFTB calculation of T_0 . When using a valence minimal basis set, the Hartree–Fock method and other semiempirical methods like PM6 provide the same energy for the T_0 irrespective of the way the latter is computed. This is not the case for DFTB, because all of the on-site exchange integrals between functions with different angular momenta vanish due to the Neglect of Differential Overlap (NDO) approximation, which makes each atomic sub-block of $S_{\mu\nu}$ diagonal. This appears to be a limitation in the current formulation of DFTB which effectively lifts the degeneracy of the three components of a triplet state.

All calculations of triplet excitation energies were performed using geometries optimized at the MP2 level, and the results have been collected in the Supporting Information. The analysis of the results does not allow for the identification of any general trend. For example, in the case of ethene, the excitation energy toward the ${}^3B_{1u}$ triplet state is predicted at 5.26 eV by TD-DFTB, while a triplet ground state calculation leads to a energy of 5.44 eV. These two results are to be compared with a TBE reference energy of 4.50 eV. In the case of formaldehyde, the singlet to triplet transition energy is computed at 4.13 eV by TD-DFTB, while the triplet ground state is at 3.71 eV and the reference value is 3.50 eV.

As in the case of the singlet excitation energies, the structural optimization by means of DFTB has a small effect, on average. The comparison with excitation energies obtained using a DFTB-optimized structures leads to 0.14 and 0.39 eV for signed and absolute error, respectively. This is in agreement with the results

obtained using the geometries optimized at the MP2 level. Also, for triplet excitation energies, the results were compared with the ones published in the previous implementation of the method,³⁶ and fair agreement (see Supporting Information) is found. Finally, it is observed that neglecting the antisymmetric contribution from $(A - B)$ has only a minor effect on the triplet excitation energies, corresponding to a change typically within 0.02 eV. Just like for singlet excited states, TD-DFTB gives good results for aromatic hydrocarbons (group II), with an overall compensation of the mean error. On the other hand, the method tends to overestimate the energies for group I molecules, but in this case, the standard deviation is small and the results are less scattered.

4. STATISTICS

In Figure 4 are shown the correlation plots of the TD-DFTB results against the TBEs, for both singlet (left panel) and triplet (right panel) excited states, for the large benchmark set of Table 1. The plots summarize the findings discussed in the previous section. Singlet vertical excitation energies are systematically underestimated within the whole range of energies considered here. The best-fit curve obtained by linear regression is parallel to the bisector, lying about 0.4 eV below it. For triplet states, the slope is slightly different, but in the energy range considered, the difference does not appear to be significant. The correlation coefficient between TD-DFTB excitation energies and TBE is $r = 0.944$ and $r = 0.940$ for singlet and triplet states, respectively. The correlation plots and the corresponding correlation coefficients are either superior or comparable with respect to the ones obtained with other semiempirical methods, such as PM3 ($r = 0.868$ and $r = 0.880$ for singlet and triplet states, respectively), INDO/S2 ($r = 0.897$ and $r = 0.796$), and OM3 ($r = 0.932$ and $r = 0.925$).⁴⁶ The high correlation coefficient shows that, in practice, the TD-DFTB singlet excitation energies do have a quality comparable to the best theoretical estimates from the literature when a rigid shift of 0.4 eV is applied.

A graphical comparison with other methods is shown in Figure 5, where the mean deviation of different methods with respect to TBEs is shown, with an error bar corresponding to the value of the standard deviation. Statistics for semiempirical methods have been taken from Thiel and Silva-Junior.⁴⁶ All of the results in black-closed symbols come from statistics performed with respect to the theoretical best estimates from the literature, over the large benchmark set of 104 singlet and 63 triplet excited states, of the organic molecules grouped in Table 1 and first proposed in ref 37. In addition, the statistics of Table 2, which refer to TD-DFTB and TD-DFT energies with respect to the experimental data, have been added to the figure as red-open symbols. They refer to a small benchmark set, but the convergence of TD-DFT results has been carefully checked by using a large basis set.⁴⁷ It is therefore included for completeness (M05 results have also been added).

As far as singlet excited states (left panel) are concerned, TD-DFTB is in fair agreement with the PBE functional. This is likely due to the fact that the DFTB parametrization of the Fock matrix has been carried out on referenced PBE calculations. TD-DFTB can undoubtedly be preferred over INDO, where significant error compensation leads to a small deviation from TBE, but the spread (the error bar in the graph) is large. Moreover, TD-DFTB appears to be more accurate than PM3, which strongly underestimates the excitation energies. Furthermore, TD-DFTB

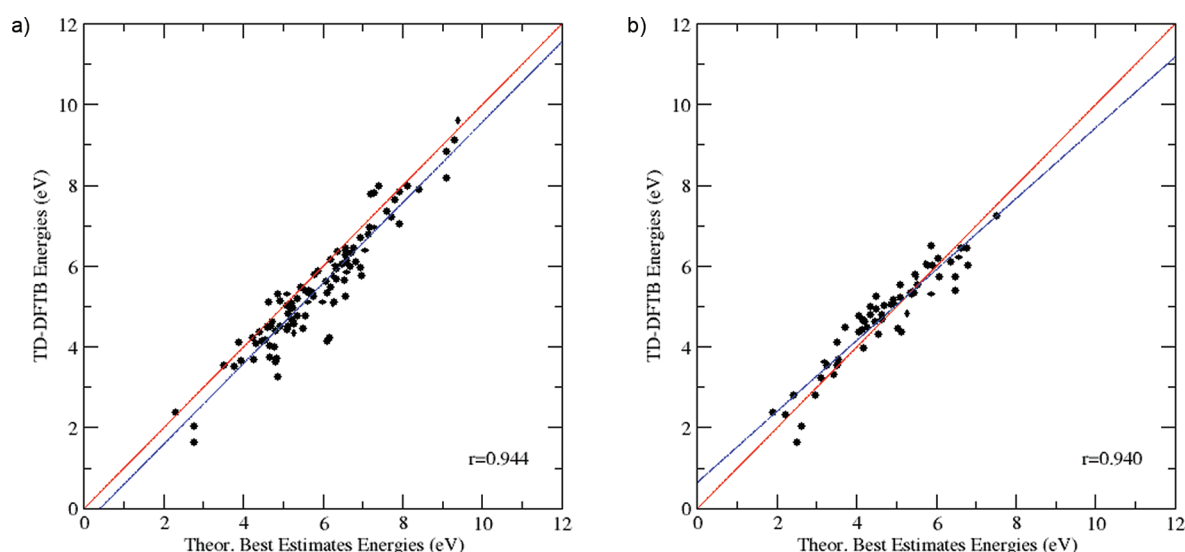


Figure 4. Correlation plots of TD-DFTB vertical excitation energies for singlet states (left panel) and triplet states (right panel) with respect to the TBEs.

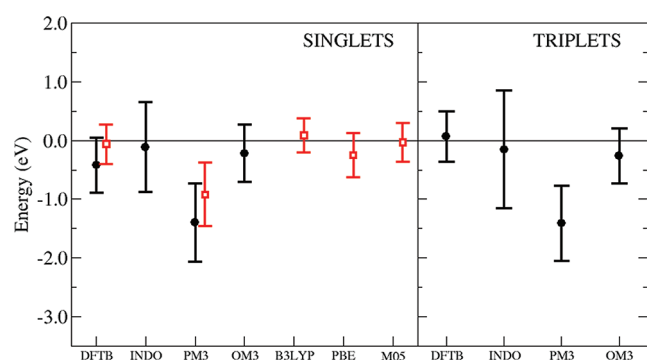


Figure 5. Graphical comparison with other methods. Black-closed symbols: mean errors of the excitation energies with respect to the TBEs, calculated for the whole benchmark set of molecules in Table 1. TD-DFTB results are compared to other results obtained from the literature, CISDTQ-PM3, INDO/S2, and OM3,⁴⁶ for singlet and triplet excited states. Red-open symbols: mean errors with respect to the experimental data of TD-DFTB, TD-PM3, TD-B3LYP, and TD-PBE data (see Table 2), calculated on a small benchmark set of excitations. TD-M05 results on the same set have been taken from ref 47.

provides results of comparable accuracy to the ones obtained by the semiempirical OM3 approach, but at a much lighter computational effort.

The comparison of the results obtained for triplet excited states is shown in the right panel of Figure 5. In the case of standard semiempirical methods, the statistics are very similar to the ones obtained for singlet states. Instead, from this figure, it is interesting to note that TD-DFTB performs better for triplet than for singlet excited states (compare TD-DFTB black-symbols, left and right panels). It has a smaller spread and a smaller signed error from TBE. It is important to remark that this is overall statistics over a large set of molecules and excited states. As was observed in the previous section (see also Supporting Information), DFTB tends to overestimate the low-lying triplet excitation energies (see Table 4), this trend being compensated from an underestimation of high-lying excitations. More than the

Table 6. Vinyl Radical Excited States (eV) Calculated by TD-B3LYP⁴⁹ and by TD-DFTB, Using the B3LYP-Optimized Geometry in Both Cases

excited state	transition	TD-B3LYP	TD-DFTB
$^2A''$	$\pi \rightarrow n$	3.29	2.84
$^2A''$	$n \rightarrow \pi^*$	4.48	4.22
$^2A'$	$\pi \rightarrow \pi^*$	4.40	4.93

mean signed error, the standard deviation (error bar in figure) is another important indicator in qualifying the goodness of a method, and TD-DFTB has a standard deviation that is much smaller than INDO and PM3 and comparable to OM3. To conclude, Figure 5 actually shows that DFTB is the best semiempirical approach, among the different models here considered, for the calculation of triplet excitation energies of organic molecules.

As a final benchmark, the excited states of the vinyl radical were calculated, as a simple case of a ground-state open-shell system, to check how TD-DFTB performs in doublet excited states calculations. A recent paper reports accurate DFT calculations of the excited states of the vinyl radical; thus we have chosen B3LYP results as a reference for TD-DFTB.⁴⁹ Among the low-lying excitations, two excited states correspond to the $\pi \rightarrow n$ and $n \rightarrow \pi^*$ transitions, while a third excited state corresponds to a $\pi \rightarrow \pi^*$ transition (note that the vinyl radical has an n -type single-occupied molecular orbital). TD-DFTB calculations were performed using the geometry optimized at the B3LYP level, and the vertical excitation energies for the first doublet states are reported in Table 6. We found an underestimation of the first ($\pi \rightarrow n$) and the second ($n \rightarrow \pi^*$) excited states by 0.45 eV and 0.26 eV, respectively. On the other hand, the A' state is overestimated by 0.53 eV using TD-DFTB.

5. CONCLUSIONS

A new formulation and implementation of the time-dependent density functional tight binding method (TD-DFTB) has

been introduced in this paper. The present scheme follows from the linear response theory applied to the DFTB ground state equations. At variance with a previously developed formulation³⁶ of TD-DFTB, the current approach does not require any additional or modified parameters for the calculation of the excited states, and it is characterized by a nontrivial antisymmetric spin contribution in the TD-DFTB equations. The current version of TD-DFTB has been benchmarked against theoretical best estimates and experimental data, from which promising results are found. It has been shown that TD-DFTB provides accurate prediction of transition energies toward both singlet and triplet excited states. To compare the method against the standard semiempirical approaches, TD-PM3 and CIS-PM3 calculations have been performed on a small set of molecules, and the results are compared to CISDTQ-PM3 results from the literature. It has been found that TD-DFTB performs better than other standard semiempirical quantum chemical methods.

■ ASSOCIATED CONTENT

S Supporting Information. All of the vertical transition energies for singlet and triplet excitations, obtained by means of TD-DFTB, using molecular geometries optimized both at the MP2 and at the DFTB level, are available free of charge via the Internet at <http://pubs.acs.org>.

■ AUTHOR INFORMATION

Corresponding Author

*E-mail: fabio.trani@sns.it.

■ ACKNOWLEDGMENT

Part of the calculations were performed using the CINECA advanced computing facilities.

■ REFERENCES

- (1) Runge, E.; Gross, E. K. U. *Phys. Rev. Lett.* **1984**, *52*, 997.
- (2) Casida, M. E. *Recent Advances in Density Functional Methods*; Chong, D. P., Ed.; World Scientific: Singapore, 1995; Vol. 1, pp 155–192.
- (3) Gross, E.; Dobson, J.; Petersilka, M. Density functional theory of time-dependent phenomena. In *Density Functional Theory II*; Nalewajski, R., Ed.; Springer: Berlin/Heidelberg, 1996; Vol. 181, pp 81–172.
- (4) Petersilka, M.; Gossmann, U. J.; Gross, E. K. U. *Phys. Rev. Lett.* **1996**, *76*, 1212–1215.
- (5) Marques, M.; Gross, E. *Annu. Rev. Phys. Chem.* **2004**, *55*, 427–455.
- (6) Burke, K.; Werschnik, J.; Gross, E. K. U. *J. Chem. Phys.* **2005**, *123*, 062206.
- (7) Dreuw, A.; Head-Gordon, M. *Chem. Rev.* **2005**, *105*, 4009–4037.
- (8) Casida, M. E. *THEOCHEM* **2009**, *914*, 3–18.
- (9) Dreuw, A.; Head-Gordon, M. *J. Am. Chem. Soc.* **2004**, *126*, 4007–4016.
- (10) Tozer, D.; Amos, R.; Handy, N.; Roos, B.; Serrano-Andres, L. *Mol. Phys.* **1999**, *97*, 859–868.
- (11) Leininger, T.; Stoll, H.; Werner, H.-J.; Savin, A. *Chem. Phys. Lett.* **1997**, *275*, 151–160.
- (12) Ikura, H.; Tsuneda, T.; Yanai, T.; Hirao, K. *J. Chem. Phys.* **2001**, *115*, 3540–3544.
- (13) Dreuw, A.; Weisman, J. L.; Head-Gordon, M. *J. Chem. Phys.* **2003**, *119*, 2943–2946.
- (14) Hirata, S.; Head-Gordon, M. *Chem. Phys. Lett.* **1999**, *302*, 375–382.
- (15) Silva-Junior, M. R.; Schreiber, M.; Sauer, S. P. A.; Thiel, W. *J. Chem. Phys.* **2008**, *129*, 104103.
- (16) Jacquemin, D.; Wathelet, V.; Perpète, E. A.; Adamo, C. *J. Chem. Theory Comput.* **2009**, *5*, 2420–2435.
- (17) Caillie, C. V.; Amos, R. D. *Chem. Phys. Lett.* **2000**, *317*, 159–164.
- (18) Furche, F.; Ahlrichs, R. *J. Chem. Phys.* **2002**, *117*, 7433–7447.
- (19) Scalmani, G.; Frisch, M. J.; Mennucci, B.; Tomasi, J.; Cammi, R.; Barone, V. *J. Chem. Phys.* **2006**, *124*, 094107.
- (20) Porezag, D.; Frauenheim, T.; Köhler, T.; Seifert, G.; Kaschner, R. *Phys. Rev. B* **1995**, *51*, 12947–12957.
- (21) Elstner, M.; Porezag, D.; Jungnickel, G.; Elsner, J.; Haugk, M.; Frauenheim, T.; Suhai, S.; Seifert, G. *Phys. Rev. B* **1998**, *58*, 7260–7268.
- (22) Cui, Q.; Elstner, M.; Kaxiras, E.; Frauenheim, T.; Karplus, M. *J. Phys. Chem. B* **2001**, *105*, 569–585.
- (23) Frauenheim, T.; Seifert, G.; Elstner, M.; Niehaus, T.; Kohler, C.; Amkreutz, M.; Sternberg, M.; Hajnal, Z.; Di Carlo, A.; Suhai, S. *J. Phys.: Condens. Matter* **2002**, *14*, 3015.
- (24) Koskinen, P.; Mäkinen, V. *Comput. Mater. Sci.* **2009**, *47*, 237–253.
- (25) Gaus, M.; Cui, Q.; Elstner, M. *J. Chem. Theory Comput.* **2011**, *7*, 931–948.
- (26) Zheng, G.; Irle, S.; Morokuma, K. *Chem. Phys. Lett.* **2005**, *412*, 210–216.
- (27) Sattelmeyer, K. W.; Tirado-Rives, J.; Jorgensen, W. L. *J. Phys. Chem. A* **2006**, *110*, 13551–13559.
- (28) Otte, N.; Scholten, M.; Thiel, W. *J. Phys. Chem. A* **2007**, *111*, 5751–5755.
- (29) Goyal, P.; Elstner, M.; Cui, Q. *J. Phys. Chem. B* **2011**, *115*, 6790–6805.
- (30) Zheng, G.; Lundberg, M.; Jakowski, J.; Vreven, T.; Frisch, M. J.; Morokuma, K. *Int. J. Quantum Chem.* **2009**, *109*, 1841–1854.
- (31) Lundberg, M.; Sasakura, Y.; Zheng, G.; Morokuma, K. *J. Chem. Theory Comput.* **2010**, *6*, 1413–1427.
- (32) Trani, F.; Barone, V. *J. Chem. Theory Comput.* **2011**, *7*, 713–719.
- (33) Zheng, G.; Witek, H. A.; Bobadova-Parvanova, P.; Irle, S.; Musaev, D. G.; Prabhakar, R.; Morokuma, K.; Lundberg, M.; Elstner, M.; Köhler, C.; Frauenheim, T. *J. Chem. Theory Comput.* **2007**, *3*, 1349–1367.
- (34) Moreira, N.; Dolgonos, G.; Aradi, B.; da Rosa, A.; Frauenheim, T. *J. Chem. Theory Comput.* **2009**, *5*, 605–614.
- (35) Dolgonos, G.; Aradi, B.; Moreira, N. H.; Frauenheim, T. *J. Chem. Theory Comput.* **2010**, *6*, 266–278.
- (36) Niehaus, T. A.; Suhai, S.; Della Sala, F.; Lugli, P.; Elstner, M.; Seifert, G.; Frauenheim, T. *Phys. Rev. B* **2001**, *63*, 085108.
- (37) Schreiber, M.; Silva-Junior, M. R.; Sauer, S. P. A.; Thiel, W. *J. Chem. Phys.* **2008**, *128*, 134110.
- (38) Kohler, C.; Seifert, G.; Gerstmann, U.; Elstner, M.; Overhof, H.; Frauenheim, T. *Phys. Chem. Chem. Phys.* **2001**, *3*, 5109–5114.
- (39) Dewar, M. J. S.; Thiel, W. *J. Am. Chem. Soc.* **1977**, *99*, 4899–4907.
- (40) Dewar, M. J. S.; Zoebisch, E. G.; Healy, E. F.; Stewart, J. J. P. *J. Am. Chem. Soc.* **1985**, *107*, 3902–3909.
- (41) Stewart, J. J. *Mol. Model.* **2007**, *13*, 1173–1213.
- (42) Stratmann, R. E.; Scuseria, G. E.; Frisch, M. J. *J. Chem. Phys.* **1998**, *109*, 8218–8224.
- (43) Slater, J. C. *Phys. Rev.* **1951**, *81*, 385.
- (44) Jacquemin, D.; Perpète, E. A.; Ciofini, I.; Adamo, C. *J. Chem. Theory Comput.* **2010**, *6*, 1532–1537.
- (45) Jacquemin, D.; Perpète, E. A.; Ciofini, I.; Adamo, C.; Valero, R.; Zhao, Y.; Truhlar, D. G. *J. Chem. Theory Comput.* **2010**, *6*, 2071–2085.
- (46) Silva-Junior, M. R.; Thiel, W. *J. Chem. Theory Comput.* **2010**, *6*, 1546–1564.
- (47) Caricato, M.; Trucks, G. W.; Frisch, M. J.; Wiberg, K. B. *J. Chem. Theory Comput.* **2010**, *6*, 370–383.
- (48) Frisch, M. J.; Trucks, G. W.; Schlegel, H. B.; Scuseria, G. E.; Robb, M. A.; Cheeseman, J. R.; Scalmani, G.; Barone, V.; Mennucci, B.; Petersson, G. A.; Nakatsuji, H.; Caricato, M.; Li, X.; Hratchian, H. P.; Izmaylov, A. F.; Bloino, J.; Zheng, G.; Sonnenberg, J. L.; Hada, M.;

Ehara, M.; Toyota, K.; Fukuda, R.; Hasegawa, J.; Ishida, M.; Nakajima, T.; Honda, Y.; Kitao, O.; Nakai, H.; Vreven, T.; Montgomery, J. A., Jr.; Peralta, J. E.; Ogliaro, F.; Bearpark, M.; Heyd, J. J.; Brothers, E.; Kudin, K. N.; Staroverov, V. N.; Kobayashi, R.; Normand, J.; Raghavachari, K.; Rendell, A.; Burant, J. C.; Iyengar, S. S.; Tomasi, J.; Cossi, M.; Rega, N.; Millam, J. M.; Klene, M.; Knox, J. E.; Cross, J. B.; Bakken, V.; Adamo, C.; Jaramillo, J.; Gomperts, R.; Stratmann, R. E.; Yazyev, O.; Austin, A. J.; Cammi, R.; Pomelli, C.; Ochterski, J. W.; Martin, R. L.; Morokuma, K.; Zakrzewski, V. G.; Voth, G. A.; Salvador, P.; Dannenberg, J. J.; Dapprich, S.; Daniels, A. D.; Farkas, O.; Foresman, J. B.; Ortiz, J. V.; Cioslowski, J.; Fox, D. J. *Gaussian Development Version*; Gaussian Inc.: Wallingford, CT, 2011.

(49) Barone, V.; Bloino, J.; Biczysko, M. *Phys. Chem. Chem. Phys.* **2010**, *12*, 1092–1101.